Journal Of Sea Research
February 2019, Volume 144 Pages 142-155
https://doi.org/10.1016/j.seares.2018.12.003
https://archimer.ifremer.fr/doc/00481/59262/

Larval supply of Peruvian scallop to the marine reserve of Lobos de Tierra Island: A modeling approach

Flores-Valiente Jorge [1, *], Tam Jorge [2], Brochier Timothee [3], Colas Francois [4], Pecquerie Laure [5], Aguirre-Velarde Arturo [6], Mendo Jaime [7], Lett Christophe [8]

[1] Universidad Peruana Cayetano Heredia (UPCH), Av. Honorio Delgado 430, Distrito de Lima, Peru
[2] Laboratorio de Modelado Oceanográfico, Ecosistémico y del Cambio Climático (LMOECC), Instituto del Mar del Peru (IMARPE), Esquina Gamarra y General Valle S/N Chucuito Callao, Peru
[3] Institut de Recherche pour le Développement (IRD), UMMISCO, Sorbonne Université, Université Cheikh Anta Diop, Campus international UCAD/IRD de Hann, Dakar, Senegal.
[4] Institut de Recherche pour le Développement (IRD), UMR LOCEAN, Sorbonne Universités (UPMC)/CNRS/MNHN, Paris 75252, France
[5] Institut de Recherche pour le Développement (IRD), UBO, CNRS, Ifremer, LEMAR, IUEM, Plouzané, France
[6] Laboratorio de Ecofisiologia Acuatica, Instituto del Mar del Peru (IMARPE), Esquina Gamarra y General Valle S/N Chucuito Callao, Peru
[7] Universidad Nacional Agraria La Molina, Av. La Molina s/n La Molina, Peru
[8] Institut de Recherche pour le Développement (IRD), Sorbonne Université, Unité de Modélisation Mathématique et Informatique des Systèmes Complexes, UMMISCO, F-93143, Bondy, France

* Corresponding author : Jorge Flores-Valiente, email address : jorgefloresvaliente@gmail.com

Abstract :

The Peruvian scallop (Argopecten purpuratus) is the second main contributor to the total catch of mollusks in Peru, after jumbo squid. There are two main scallop banks populations in northern Peru: Lobos de Tierra Island (LTI) and Sechura Bay (SB). Despite a continuous, intense relocation of seeds from LTI, the natural bank population still persists there. To understand this, we studied larval connectivity between LTI and SB using the first invertebrate larval transport biophysical model developed in the region. Larval local retention were 2.4% and 1.57% on average at LTI and SB respectively, while larval transport from SB to LTI was 0.02% on average and 0.07% in the opposite direction. Both larval retention and larval transport increased with spawning depth and were highest in austral summer. Two main larval transport paths from SB to LTI were identified, resulting from a combination of horizontal mesoscale circulation patterns and vertical flows. Potential management implications for these natural banks are discussed.

Highlights

► Larval transport model of Peruvian scallop simulated retention and transport between two natural banks in Northern Peru. ► Larval retention and larval transport of Peruvian scallop increased with spawning depth and were highest in austral summer. ► Larval transport paths between the two natural banks depended on complex mesoscale circulation patterns and vertical flows. ► Daily and monthly wind forcings changed simulated mean larval transport but retention was not affected. ► Restoration and maintenance of both natural banks will improve sustainability of aquaculture activities.

Keywords : Peruvian scallop, Larval transport, Biophysical model, Marine connectivity, Marine reserve, Humboldt Current System

1. INTRODUCTION

The Peruvian coastal upwelling system has been classified as a highly productive Large Marine Ecosystem (Kämpf and Chapman, 2016). This ecosystem supports many different industrial and artisanal fisheries targeting fishes, crustaceans and mollusks. Mollusks, especially bivalves, are traditionally exploited in Peru by the artisanal near-shore diving fishery. In particular, the Peruvian scallop (*Argopecten purpuratus*) has become the most important contributor (43,657 tons) to the total catch of mollusks (535,433 tons) excluding jumbo squid (460,010 tons) in the period from 2006 to 2015 (PRODUCE, 2016). Due to its high demand in international markets and its culture intensification, *A. purpuratus* has become an important commercial species for artisanal fisheries in Peru (Mendo, 2009; Mendo et al., 2016).

Since the 1980's, *A. purpuratus* has been successfully cultured in bays and semi-enclosed areas, mainly in Sechura Bay (SB, 5.5°S) in the North of Peru, and previously in Independencia Bay (14°S) in the South of Peru (Kluger et al., 2018; Taylor et al., 2008; Wolff, 1988). Cultures techniques consist in artificially boosting the population in natural habitat by bringing supplementary post-larval individuals, called "spats" (<10mm) or "seeds" (10-30 mm). While the spats are normally obtained from artificial hatcheries or planktonic larval collectors deployed at sea, seeds are already settled individuals collected in natural habitat, relocated into the aquaculture concession area. Although relocation of seeds from Natural Reserves is forbidden in Peru, it has been recently reported from the Lobos de Tierra Island (LTI, 6.5°S) natural banks to

SB (Mendo et al., 2016; Kluger et al., 2018). Thus, in Peru the supply of individuals for culture activities currently depends almost entirely on the availability of natural populations, due to the elevated costs of hatchery and larval collectors.

In addition, catches of *A. purpuratus* are inherently unpredictable due to the high environmental variability and the many abiotic factors that may affect scallop larval and adult stages and therefore recruitment (Wolff et al., 2007). While scallop biomass is enhanced by El Niño events in southern Peru and northern Chile (Stotz, 2000; Wolff, 1987), in northern Peru, moderate and strong El Nino Events have negative effects on scallop populations. During El Nino, there is a high precipitation in northern Peru with increased flow of rivers that carry large amounts of sediments which are dischargerd to the sea causing a decrease in salinity. In addition, turbidity and low salinity cause high mortality of scallops in summer months (Cisneros, 2012; Taylor et al., 2008).

It is generally accepted that scallop recruitment, like for many other benthic populations (Pineda, 2000; Pineda et al., 2007), relies heavily on larval retention and transport processes. Indeed, mollusks marine larvae are very small, spent most of time as part of the plankton and cannot overcome the turbulence and currents. Thus the use of larval tracking models has been quite satisfactory to represent their spatial distribution focusing on connectivity, analyzing the larval flow between zones (Gilbert et al., 2010; Munroe et al., 2018; Tian et al., 2009b, 2009a). Other authors applied a model for a whole life cycle including larval transport and bioenergetics submodels being able to reproduce its population dynamics (Le Goff et al., 2017). However both experimental and modeling studies focusing on bivalves are very scarce in

South America (Bryan-Brown et al., 2017). In fact, there has been no study to date about *A. purpuratus* larval transport in Peru, despite LTI and SB are sufficiently close to each other to have significant larval connectivity (Mendo, 2009).

Since 2009, LTI has been included in the National Reserve System of Islands, Islets and Guano Capes (MINAM, 2009). However the natural banks of LTI have been subject to a continuous extraction of scallops of all sizes (Mendo, 2009). The extraction increased as the market developed, together with the intensification of aquaculture activities in SB, particularly in the early 1990s with the onset of diving techniques (Taylor et al., 2008). Extracted adults are commercialized but juveniles are relocated mainly to SB, for on-growing purposes (Mendo, 2009). Figure 1 shows the biomass and abundance of scallops in LTI and SB over the period 1995-2015 from Instituto del Mar del Peru (IMARPE) surveys (Carbajal et al., 2005, 2004; Ramirez et al., 2016). The scallop biomass around the island showed moderate interannual peaks, with a relatively stable long-term trend. In contrast, the scallop biomass in the bay showed stronger fluctuations with two moderate peaks in 1997-1998 and 2007-2008, and a large peak in 2010-2011, the latter being boosted by the aquaculture boom. The average scallop abundance between 2007 and 2015 in SB reaches 1340 million, approximately 4.5 times higher than in LTI (292 millions). The increase of aquaculture demand for seeds caused the relocation of juvenile individuals from LTI to SB, which facilitated the increase of the population in the bay since 2007 (Mendo, 2009), indeed the average proportion of juveniles in LTI since 1995 to 2014, has been 76 %, what evidence the translocation activities (Mendo, pers. comm.). Given the continuous, intense

relocation of seeds from LTI since more than a decade, one could have expected the extinction of this population, but the natural bank population still persists there (Figure 1).

On the other hand, the complexity of the tridimensional circulation dynamics in northern Peru could allow several potential pathways from SB to LTI and vice-versa. In northern Peru the surface layer is dominated by the equatorward flow parallel to the coast (Peru Coastal Current, PCC); below this current, a poleward flow dominates the subsurface and the shelf (Peru Chile Under-Current, PCUC; Penven et al., 2005).

Within this context we postulate that both larval local retention near the island and larval transport from SB contributes to the maintenance of LTI natural banks. Understanding the relative contributions of retention and transport is a prerequisite for sustainable management. This issue is addressed hereafter using a biophysical larval transport model coupled to a 3D hydrodynamical model, at a high spatial resolution (2.2 km) to quantify numerically larval drift from SB to LTI and local retention around LTI.

METHODS

The model description follows the ODD (Overview-Design-Details) protocol for describing individual-based models (Grimm et al., 2010, 2006).

1.1. Purpose

In order to understand which factors determine the persistence and maintenance of the Peruvian scallop (*A. purpuratus*) population at LTI, despite the relocation of juveniles to SB, we used the Ichthyop biophysical model (Lett et al., 2008) to assess the larval local retention around the island and the larval transport from the bay to the island and its main trajectories. The same approach was applied to for larval retention at SB and larval transport from LTI to SB.

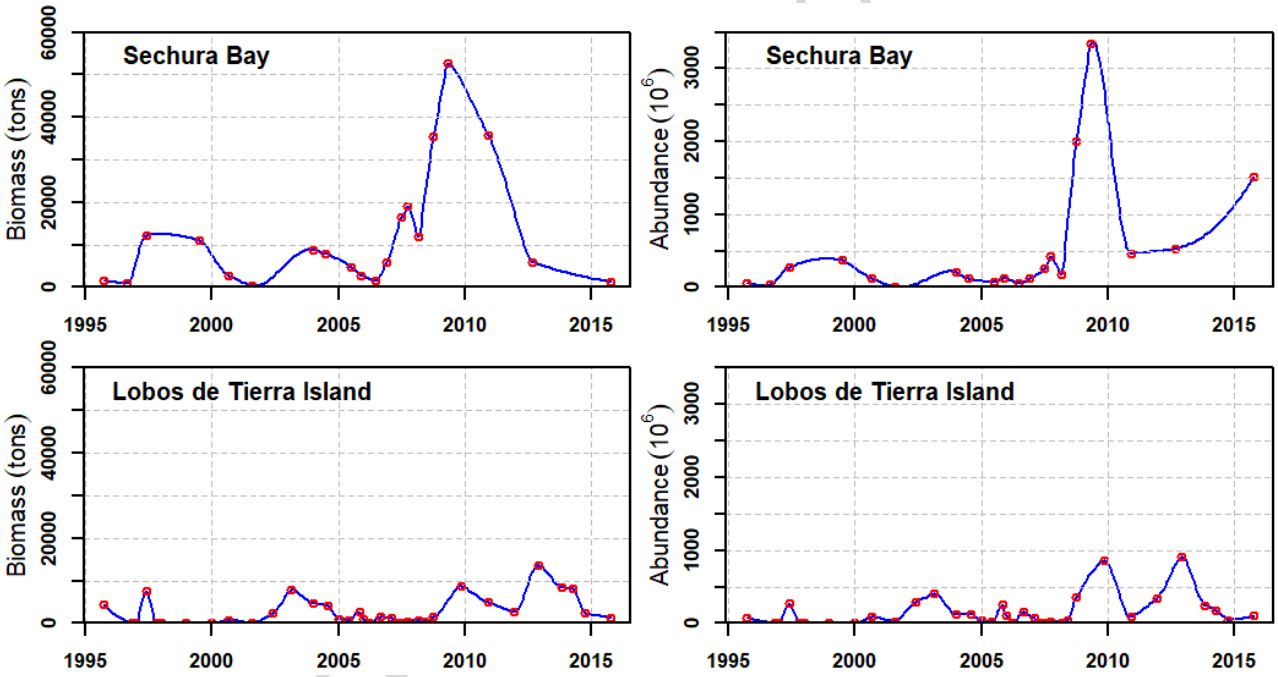

Figure 1 Time series of scallop biomass (tons; left column) and abundance (millions; right column) in Sechura Bay (top row) and Lobos de Tierra Island (bottom row) interpolated (blue curves) from IMARPE surveys data (red open circles).

1.2. Entities, state variables and scales

The model included two types of entities, the individuals and the environment. Each individual was characterized by state variables: age (in days), location (in 3D, longitude, latitude and depth) and status (ready/not ready

to settle). The environment was characterized by 3D fields of state variables: ocean current velocities (m/s) provided by archived hydrodynamic simulations. The hydrodynamic model used was the Regional Ocean Modeling System (ROMS; in its AGRIF version 3.0, https://www.croco-ocean.org/). ROMS resolves the hydrostatic primitive equations of the ocean dynamics and uses terrain-following curvilinear vertical coordinates (Shchepetkin and McWilliams, 2005). The model grid extends from 4.5 °S to 16 °S along the Peruvian coast to ~800 km offshore with a horizontal resolution of approximately 2.2 km and 42 vertical levels in sigma-coordinates. Vertical mixing processes were parameterized, in the ROMS model, by a non-local, K-profile planetary (KPP) boundary layer scheme (Large et al., 1994). The bottom topography was interpolated from the SRTM30 database (Becker et al., 2009). This domain was nested offline (following the method described in Mason et al. 2010) in a ROMS model climatological solution of the South-Eastern Pacific with an horizontal resolution of 7.5 km, described and validated in Colas et al. (2012). The 2.2 km resolution model was run for five years. It was forced with Advanced Scatterometer (ASCAT) daily wind stress at 1/4 ° resolution (Bentamy and Fillon, 2012) for the period between 2008 and 2012. Other atmospheric fluxes forcing were from the Comprehensive Ocean Atmosphere Data Set surface fluxes monthly climatology at 1/2 ° resolution (COADS; Da Silva et al., 1994). Very similar model solutions are presented in McWilliams et al. (2009) and Thomsen et al. (2016), and are shown to adequately resolve the near-coastal circulation (i.e. the surface equatorward Peru Coastal Current [PCC] and the subsurface poleward Peru-Chile Undercurrent [PCUC]), and the (sub) mesoscale activity in the region. Note that we performed another ROMS

simulation, differing from the simulation described above only by its wind forcing. In this second hydrodynamic simulation, we used a monthly climatology of ASCAT wind stress for the period 2008-2012. Comparing particles advection patterns obtained with this two different simulations gives us a sense of the sensitivity of our results to the wind frequency forcing and their robustness.

Since the model reached a statistical equilibrium after a spin-up of 2 years, we used the last 3 years, out of five, of the ROMS climatological simulation to run Ichthyop simulations. Ichthyop model used a Lagrangian particle tracking trilinear interpolation scheme (Arakawa C-grid), in time and space, using a forward Euler numerical scheme every two hours to calculate values of the physical state variables at any individual location. A horizontal diffusion scheme was applied according to Peliz et al., (2007) and the vertical movement comes only from advection. In this horizontal scheme K_h is the imposed explicit Lagrangian horizontal diffusion of the form:

$$K_h = \varepsilon^{1/3} l^{4/3}$$

; where l is the unresolved sub-gridscale (here taken as the cell size, ~2200 m) and $\varepsilon = 10^{-9}\, m^2/s^3$, is the turbulent dissipation rate (e.g., Monin and Ozmidov, 1985). This gives a K_h = ~28 m^2/s. Note that a sensitivity test with other values for ε was also performed ($from\ 10^{-8}\, m^2/s^3\ to 10^{-10}\, m^2/s^3$), leading to a K_h = ~ 10 m^2/s (which is the value used in Lindo-Atichati et al., 2016) and the seasonal patterns for larval retention and transport, changes in the intensity of retention and transport did not change significantly. So overall we are confident that the parameterization used in our study is rather adequate.

The age of a larva was used in the model to determine if it was ready to settle within a recruitment area, but we did not considered its vertical position in

the water column. We assumed that aged larvae would be able to settle, either close to the bottom or near the surface, because the final average depth of retained particles was aroung 20 m and the recruitment area at LTI is relatively shallow (mean depth ~18 m). In addition, settling velocities have been reported in a range of 0.6 to 2 mm/s for other species of bivalves (Mann et al., 1991) which allow a fast settlement in shallow areas.

The duration of each simulation was 25 days, encompassing the maximum duration of the larval period for Peruvian scallop (Cragg, 2016; Mendo et al., 2016; von Brand et al., 2006).

1.3. Process overview and scheduling

Virtual individuals were released in the environment following a determined spatial (area and depth) and temporal (month and minimum age to settlement) spawning strategy that constituted the initial conditions (see Section 2.5). After spawn, each individual was advected by currents every time step until ready to settle. Depending on the type of simulation (Table 1, Simulation I and III), the release zone and settlement zone were the same (for larval local retention around LTI or SB respectively) or were different (Table 1, Simulation II and IV, for larval transport from the SB to LTI and in the opposite direction respectively). In this study, the individuals were considered as neutrally buoyant and with a passive behavior given the limited capacity of movement of scallop larvae during their pelagic period (Cragg, 2006, 1980).

1.4. Design concepts

The model is based on the concepts of larval “local retention” defined as the ratio of locally produced settlement to local egg production (Lett et al.,

2015); “larval transport” defined as the horizontal translocation of a larva between points X_1,Y_1 and X_2,Y_2, where X and Y are horizontal axes (Pineda, 2000; Pineda et al., 2007) and “larval supply” defined as the concentration of competent larvae at a retention zone (Jonsson et al., 2004). Because it is not possible to simulate all larvae due to computational power limitation, we transformed the relative larval local retention and larval transport success rates to absolute number of larvae based on the observed abundance multiplied by the fecundity of *A. purpuratus* ($3.8 * 10^6$ eggs per spawning individual) (Aguirre-Velarde, 2016). The observed abundance is considered as the adult population, as maturity is attained by individuals from approximately 25 mm shell height (Mendo et al., 1989), which results in $5.09 * 10^{15}$ larvae/particle for SB, representing a greater number of larvae than LTI ($1.11 * 10^{15}$ larvae/particle). Finally, in order to include the concept of metapopulation (Hanski and Gilpin, 1991) as the set of local populations which interact via individuals moving among populations, we carry out two additional simulations (Table 1, Simulation III and IV) to evaluate larval local retention at SB and larval transport from LTI to SB.

1.5. Initialization

At the beginning of each simulation, 20,000 particles were released randomly over the corresponding spawning areas. We tested (not shown) the number of released particles (from 5000 to 50000 particles) and the time step of the model (from 10 minutes to 2 hours) and finally we found that a time step of 2 hours with 20000 particles gave stable results among repeated simulations.

The LTI spawning zone was defined as the eastern side of the island, from 6.33 °S to 6.5°S with a bathymetry limited by 60 meters. Indeed, only the

eastern part of the island is sheltering scallop population, the western part being too much exposed to waves (Arguelles, pers. comm.). The SB spawning zone was defined from 5.16 S° to 5.91 S° with a bathymetry limited by the 60 m isobath (Figure 2).

The initial conditions of virtual spawning were defined by spawning year (in climatological sense), month, depth and minimum age to settlement (Table 1). Three levels of spawning depths (0-15 m, 15-30 m, 30-45 m in LTI and 0-10 m, 10-20 m, 20-30 m in SB) were tested within the range occupied by adults of *A. purpuratus* during the spawning season (spring-summer; Cisneros, 2012; Mendo et al., 2016). Based on estimates for pelagic larval duration (PLD) obtained from a private laboratory in SB (15 to 20 days by Mendo et al., 2016) and from pectinid literature (16 to 25 days by von Brand et al., 2006) we tested three values of minimum age of settlement (15, 20 and 25 days). Due the high resolution and variability of the model, there is the possibility of sampling retention structures just after spawning, so we set up 3 different spawning dates within each spawning month ($1^{st,}$ 10^{th} and 20^{th}) and then we averaged results for each month. The larvae were considered as purely passive Lagrangian particles in the model, as for scallops larvae the movement is believed to be very limited (Cragg, 2006, 1980). For simplicity, the effect of mortality is neglected in the larval transport model, since we mainly focus on the transport and retention routes rather than the population dynamics.

1.6. Observation

We evaluated the impact of passive transport by currents on the larval supply to LTI, defined here as the concentration of competent larvae (Jonsson

et al., 2004) arriving at the settlement area. To do so, larval local retention (at LTI) and larval transport (from SB) were calculated.

1.7. Simulation experiments and sensitivity analyses

We carried out four simulations experiments (Table 1): simulation I and simulation II to assess larval local retention at LTI and larval transport from SB to LTI; additionally, simulation III and simulation IV to assess larval retention at SB and larval transport from LTI to SB; sensitivity analyses were performed in order to test the effect of different spawning strategies (spawning year, spawning month, spawning depth and minimum age to settlement) and their first degree interactions. Statistical significance of each factor was assessed with a Permutational Analysis of Variance (PERMANOVA), as the data were not normally distributed according to Anderson test (not shown).

RESULTS

1.8. Hydrodynamic simulations

ROMS simulations off Northern Peru reproduced known circulation patterns: surface outflows exit SB by the northern part, with speeds between 0.05 and 0.20 $m.s^{-1}$, while subsurface inflows enter SB by the central part (under 10 m depths) towards southeast, with speeds of 0.15 $m.s^{-1}$. Vertical profile presented strong near-surface currents (up to 0.20 $m.s^{-1}$ at 10 m) and weaker currents in deeper layer (about 0.05 $m.s^{-1}$ at 30 m) (Figure 3, upper panels). The PCC also showed a seasonal pattern reaching a minimum velocity during austral summer and fall, and a maximum in austral winter (Figure 3, bottom panel). PCC also showed a seasonal pattern reaching a minimum velocity during austral summer and fall, and a maximum in austral winter (Figure 3, bottom panel).

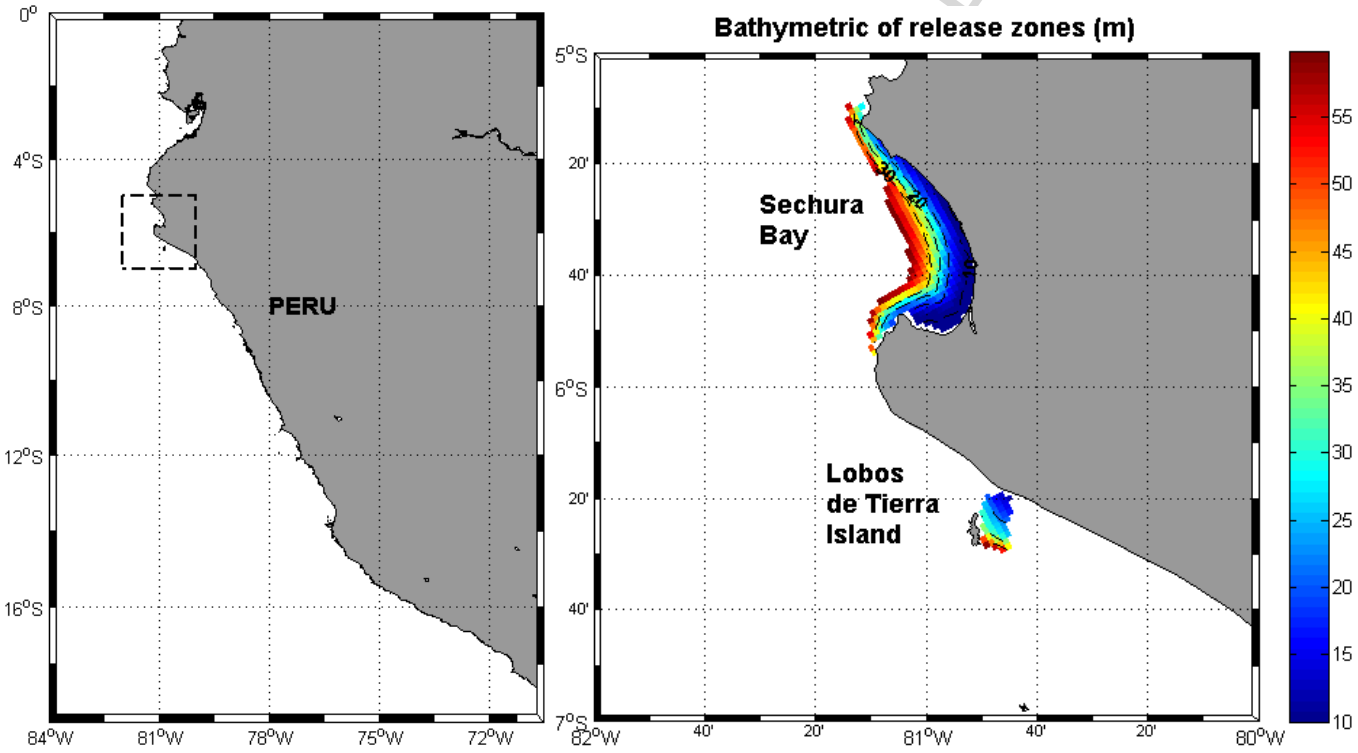

Figure 2 Left panel: the northern Peru domain where simulations for scallop larval transport were performed. Right panel: location and bathymetry of the Sechura Bay (top) and Lobos de Tierra (bottom) areas used for scallop

release and recruitment (see text for details). Isolines represent the ROMS model bathymetry.

Figure 3 Annual mean current intensity (m/s) showing a northward flow at 10-meter depth (upper-left panel) and southward flow at 30-meter depth (upper-right panel). The lower panel figure shows monthly means of alongshore current velocity (m/s) vertical profile, averaged over the area defined by the black square on the top panel figures. Under 20 meters depth, the particles can reach currents favorable to transport toward the island. Hydrodynamical model simulation was forced with daily winds.

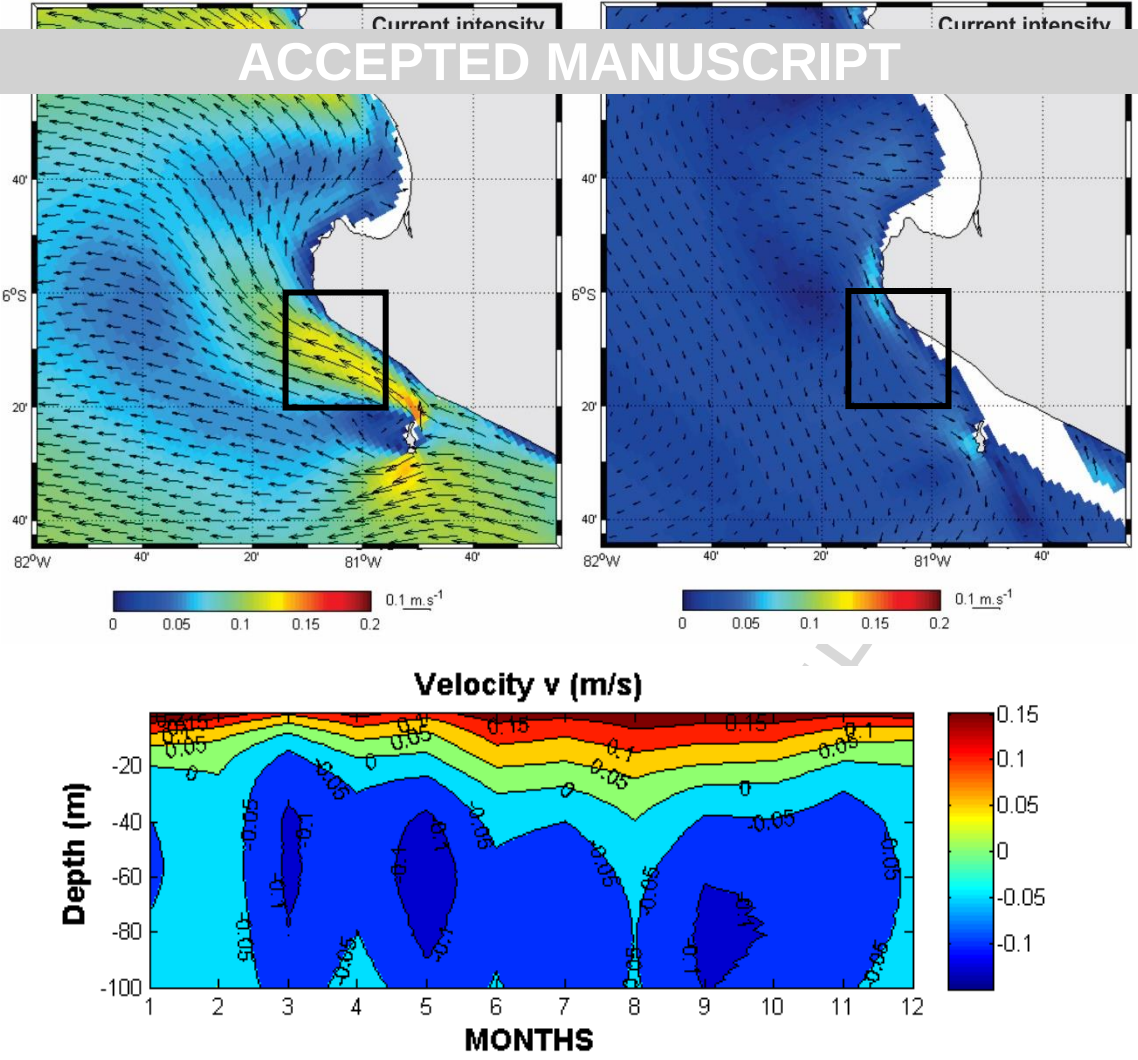

Larval retention at LTI

The results of Simulation I experiment revealed larval local retention around LTI (mean 2.4 %) and showed that the factors affecting significantly ($p < 0.05$) simulated larval local retention at the LTI in decreasing order of variance contribution were (Figure 4, upper panels; Table 2): spawning month (20.7 %), spawning depth (19.1 %), and minimum age to settlement (6.7 %); spawning year was significant, but with very low variance contribution (0.3 %).

Particles released at 30-45 m had higher local retention values (5.6 % on average) than those released shallower at 0-15 m (0.08%). Larval local retention at the island showed a strong seasonal pattern with higher values in Austral summer (December to April) and a peak (7.6 %) in March. As expected, particles with a lower minimum age to settlement (15 days) were more

frequently locally retained (4.2 %) than those with minimum age to settlement of 20 days (2.2 %) and 25 days (0.9 %).

A general pattern of counterclockwise trajectories for local retained particles near LTI was observed: particles leave the southern part of the island, deepen and go southward in the PCUC and shortly after are upwelled into the shallow PCC northward current (Figure 5, upper panel). There was also a clear deepening pattern of particles retained at the island in their first ~8 days (Figure 6, upper panel, red lines), followed by a shallowing pattern afterwards. These features did not occur for non-retained particles, which stayed on average close to their release depth (Figure 6, upper panel, upper panels, blue lines). The maximum distance between the retained particles and the LTI was larger from February to July (23.8 km) and was shorter from August to January (18.22 km).

Figure 4 Simulated larval local retention at LTI (upper panels) and larval transport success from SB to LTI (lower panels) for different spawning months, different spawning depth levels and different minimum ages to settlement. Red lines represent the seasonal pattern of Gonadosomatic Index (GI) of *A. purpuratus* according to Cisneros (2012).

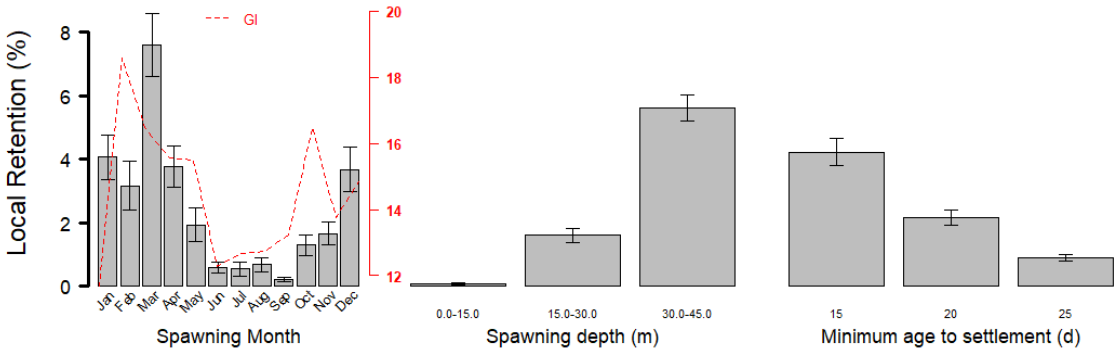

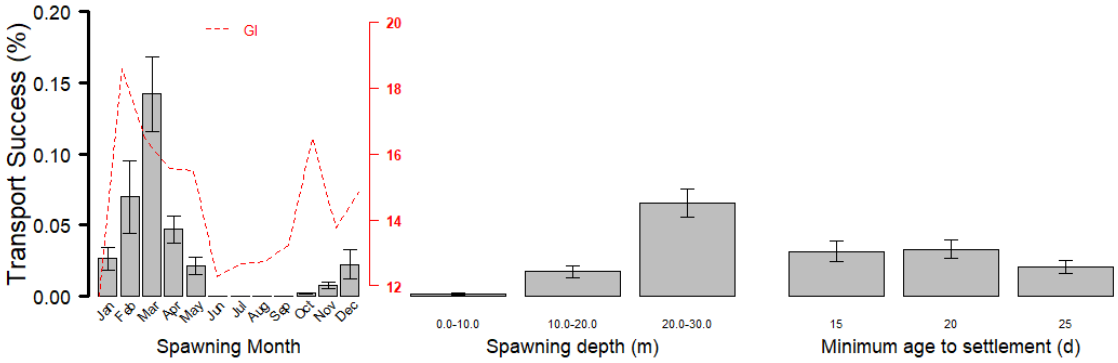

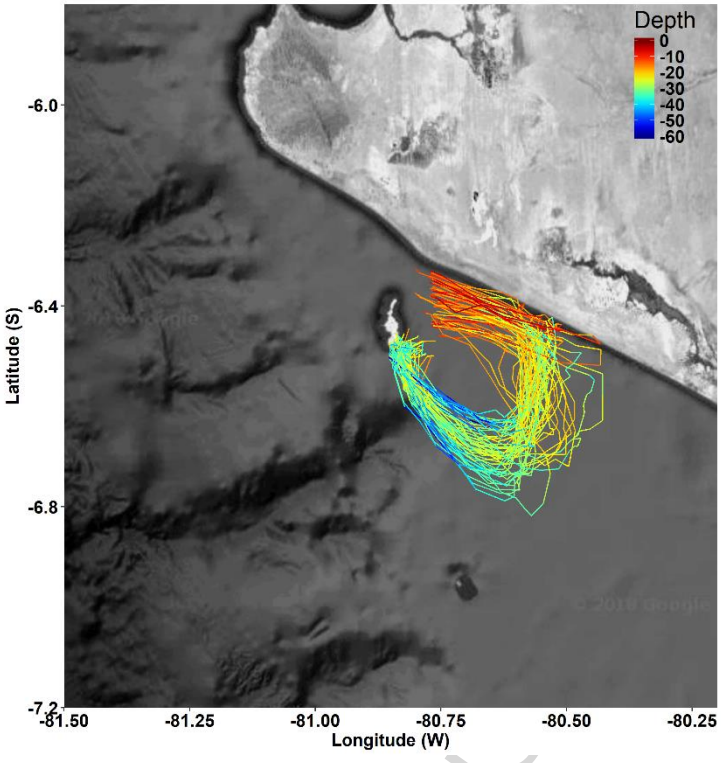

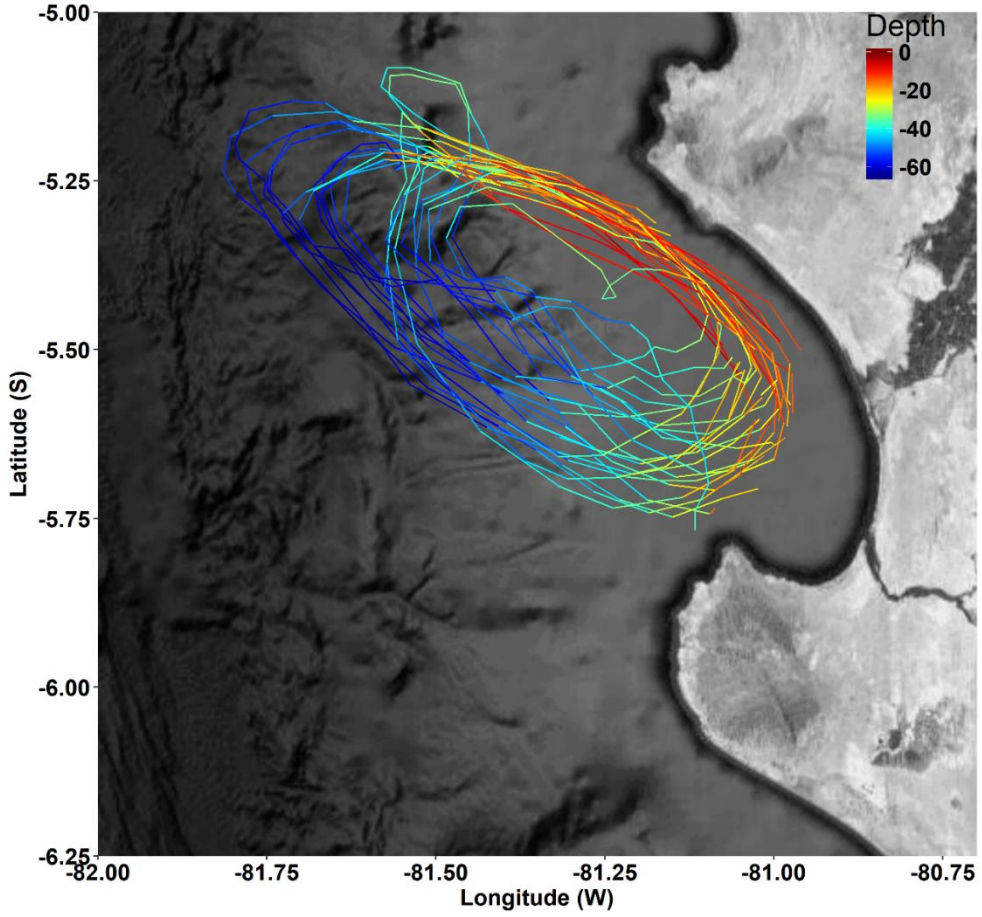

Figure 5 Random sample of 60 and 40 typical counterclockwise trajectories

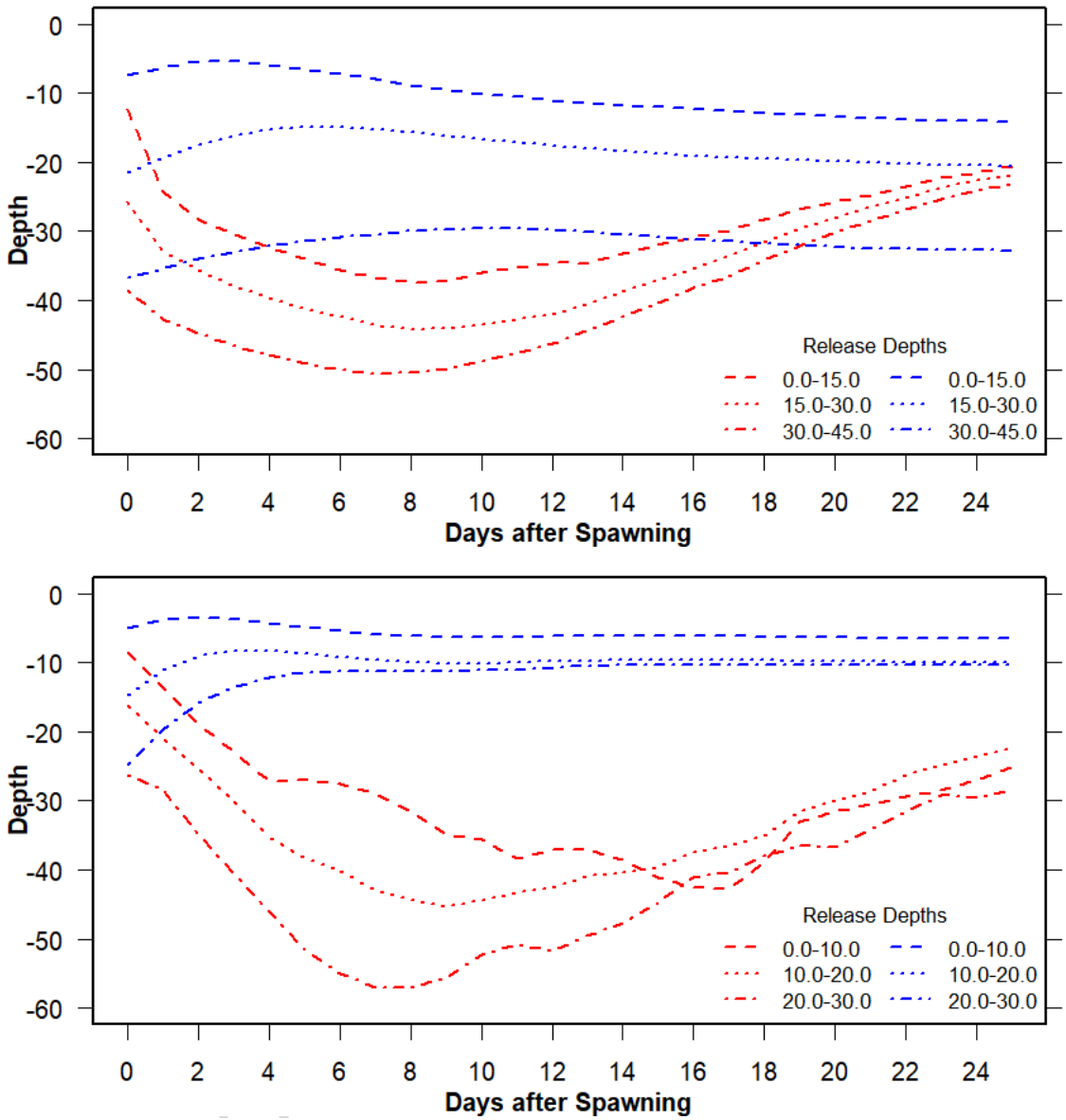

followed by particles locally retained at LTI (upper panel) and SB (lower panel) respectively.

Figure 6 Upper panel: Time evolution of the daily-average depth of retained particles (red lines) and non-retained particles (blue lines) around LTI (upper panel) for three different release depth levels. Lower panel: Time evolution of the daily-average depth of successfully transported particles (red

lines) and unsuccessfully transported particles (blue lines) from ST to LTI (lower panel), for three different release depth levels.

1.9. *Larval transport from SB to LTI*

The results of Simulation II experiment revealed larval transport success from SB to LTI (mean 0.02 %) and showed that the factors affecting significantly simulated larval transport success from SB to LTI, in decreasing order of variance contribution, were (Figure 4, lower panels, Table 3): spawning month (20.8 %) and spawning depth (7.2 %). Minimum age to settlement did not have a significant effect on larval transport success; spawning year was significant, but with very low variance contribution (1 %).

Transport success showed a strong seasonal pattern, similar to retention, with higher values in summer (Feb-Apr) and a peak in March (0.14 %). However, monthly values of larval transport success were much lower (< 0.14%) than local retention values (~ 2.4 %), and close to zero in winter (June to September). Particles released deeper (20-30 m) reached higher local retention values (0.06 %) than particles released shallower (0-10 m, 0.001 %).

Two predominant paths of particles transported from the bay to the island were observed in the simulations: (i) particles leave SB from its southern part, then deepen to southward subsurface currents and remain close to the coast, until they are recruited in the north-eastern part of the island (Figure 7, upper panel, label 1); and (ii) particles from the southern part of SB pass through the western part of the island to its southern part where they encounter upwelling which rise them up, allowing them to return north-westward to the island through surface currents (Figure 7, upper panel, label 2). Another less common

type of trajectory (iii) occurred in ~ 1 % of the cases: particles leave SB from its northern part, where downwelling flows drive them southward by subsurface currents and then they follow a path similar to trajectory (ii) (Figure 7, upper panel, label 3). The first two types of paths occurred approximately in similar proportions (Figure S1, left panel).

A deepening pattern occurred for successfully transported particles in the 7-17 first days of their trajectories (depending on release depth), followed by a shallowing pattern (Figure 6, lower panel, red lines), similarly to the retention pattern. Successfully transported particles reach subsurface southward currents, while unsuccessfully transported particles remain at the surface and were advected northward (Figure 6, lower panel, blue lines). The average distance traveled from the bay to the island by successfully transported particles was calculated as 98 km (which is 1.3 times larger than the linear distance) and it showed a seasonal pattern opposite to larval transport.

1.10. Larval retention at SB

The results of simulation III, revealed larval local retention within SB (mean 1.57 %) with the same seasonal pattern as LTI, but lower retention rates. Factors affecting significantly ($p < 0.05$) simulated larval local retention in SB in decreasing order of variance contribution were (Table 4): spawning month (9.6 %), spawning depth (8.2 %), and minimum age to settlement (4.3 %); spawning year was significant, but with very low variance contribution (1.5 %). One predominant path of particles retained near SB was observed: particles leave outside the bay by its northern part, deepen through southward countercurrents and travel back to the bay advected by shallow northward currents (Figure 5, lower panel).

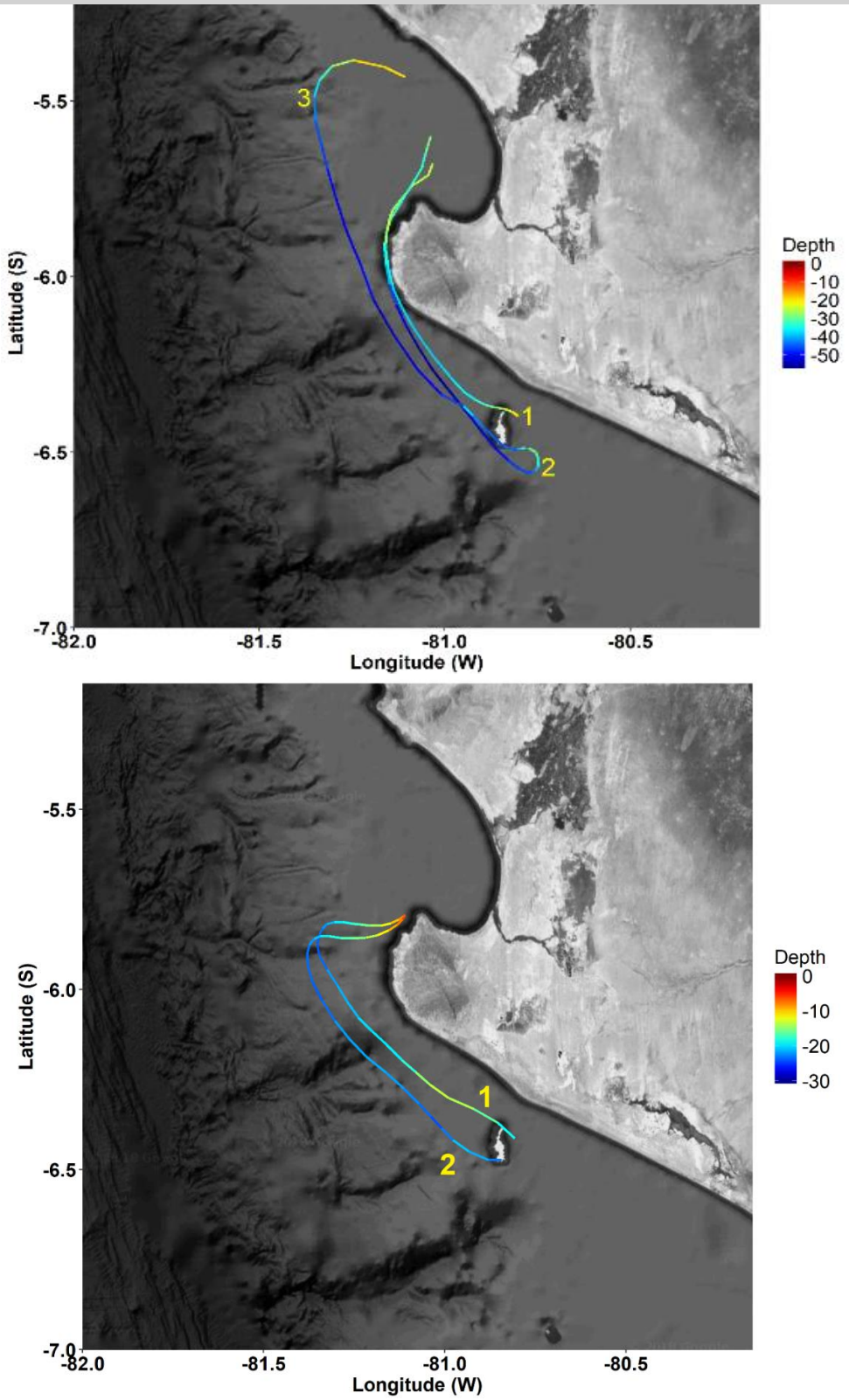

Figure 7 Upper panel: Mean trajectories of particles transported from Sechura Bay to Lobos de Tierra Island illustrating the three observed paths: (1) through the eastern part of the island, (2) through the western and southern part of the Island, and (3) less common trajectory from the northern part of the bay. Lower panel: Mean trajectories of particles transported from Lobos de Tierra Island to Sechura Bay illustrating the two observed paths in our simulations: (1) through the eastern part of the island and (2) through the western part of the Island.

1.11. Larval transport from LTI to SB

Results of simulation IV revealed that larval transport from LTI to SB is also possible (mean 0.07 %), with a similar seasonal pattern as larval transport from SB to LTI, however the transport mechanisms require further studies. In addition, the factors affecting significantly simulated larval transport success, in decreasing order of variance contribution, were (Table 5): spawning month (13.7 %) and spawning depth (1.5 %). Minimum age to settlement did not have a significant effect on larval transport success; spawning year was significant, but with very low variance contribution (0.5 %); see more details in supplementary material. The highest larval transport success from the island to the bay occurred at medium spawning depths (15-30 m), where particles can reach shallower northward currents. However, they do not travel deeper (as from the bay to the island) because of the southward undercurrent. Two predominant paths of transport from the island to the bay were found (Fig. 11): (i) particles leave the northern part of the island and are transported near the coast at medium depths and enter by the southern part of the bay and (ii) particles leave the southern part of the island and are transported far from the coast and then merge with the particles of the first trajectory to enter the bay (Figure 7, lower panel).

1.12. Larval supplies to STI and to SB

Taking into account that the Peruvian scallop biomass in the bay is approximately 4.5 times higher than in the island (De La Cruz et al., 2006; Mendo, 2009), the relative seasonal values of larval retention (mean 2.4 %) and transport success (mean 0.02 %) were expressed as absolute contributions to LTI larval supply from larval retention (mean 94.9 %) and larval transport (mean

5.1 %). Similarly, absolute contribution to SB larval supply came from larval retention (mean 99.5 %) and larval transport (mean 0.5 %).

1.13. Effects of wind forcing frequency

We compared larval retention and transport results using two hydrodynamic model simulations differing only by the frequency of their wind forcing (i.e. using monthly wind averages and daily wind values). Mean larval

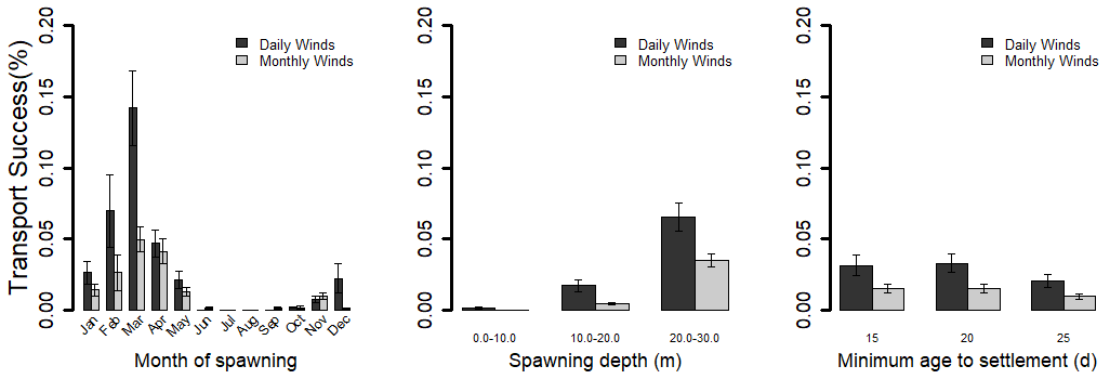

Figure 8 Comparison of larval transport from Sechura Bay to Lobos de Tierra Island between simulations forced by daily wind (dark bars) and by monthly climatological wind (light bars). The larval transport pattern is similar in the two simulations, however the amount of successfully transported particles is twice larger in the simulation forced by daily wind.

local retention values around the island were similar for both wind frequencies (2.4 % for daily winds; 2.5 % for monthly winds), but mean larval transport values from the bay to the island was double for daily winds (0.028 %) compared to monthly winds (0.014 %) (Figure 8).

DISCUSSION

1.14. Hydrodynamic simulations and wind forcing effects

This is the first biophysical larval transport model for Peruvian scallop, using high spatial resolution (2.2 km) and high frequency wind forcing (daily winds). Sensitivity studies with biophysical larval dispersal models are necessary to explore the complexity of abiotic and biotic factors affecting the early life stages of marine organisms (Miller, 2007). Peck and Hufnagl (2012) emphasized the need to include a formal sensitivity analysis when using biophysical larval dispersal models, before increasing the complexity of the model by including new processes. In this sense we carried out sensitivity analyses with different release months (12 months), release depths (up to 15 m, 30 m and 45 m) and minimum ages to settlement (15, 20 and 25 days). Then, the hydrodynamic model simulation used here represented the general features of the near-coastal circulation, such as the surface equatorward Peru Coastal Current (PCC), the subsurface poleward Peru Chile Under Current (PCUC) and the associated mesoscale eddy dynamics (see Colas et al. 2012 and Thomsen et al. 2016 for elements of validation against observations). Observations of the circulation in the SB and LTI areas are relatively scarce and insufficient to provide an in-depth validation of the model simulation in the local study area, however Morón et al. (2013; not shown) characterized the hydrodynamics of SB, finding circulation patterns of inflow and outflow similar to our model simulations. *In-situ* data of scallop larvae abundance are also very scarce for Northern Peru, however Fiestas et al. (2009 cited by Mendo et al. 2011) reported larval densities in SB, finding higher larval densities in the Southern part of the bay, similar to our simulation of larval retention at SB (Fig. 2 in SI).

The wind forcing frequency used in the model can also play an important role in larval transport simulations. These differences indicate a greater

complexity in the process of larval transport from the bay to the island compared to the process of local retention in the island, and suggest that for larval transport between two very coastal areas, models at high spatial resolution may be very sensitive to the wind frequency forcing. For example, upwelling south of the island was more intense when using daily winds (Figure 9, left panels), which explains the greater transport from the bay to the island in the simulations forced by daily winds (Figure 9). In addition, for larval transport from the bay to the island, there were differences in the interaction strength between year-month, which explained 11.3% of the variability using daily winds, and only 5% using monthly winds. Thus high frequency of winds can generate significant differences in larval transport rates. This is in line with Liu et al. (2015) who also found a strong effect of the local wind variability on scallop larvae transport (although at a larger scale).

1.15. *Processes controlling local larval retention and transport success*

Local larval retention and transport depended on several factors. Simulation I and III showed that highest local larval retention values at LTI and SB were obtained at deeper spawning depth in summer due to the presence of weaker currents than in shallow depths. At deeper levels, the current intensity was generally lower (Figure 3, upper panels). The interactions of month-depth factors for larval retention explained 13.03 % of the variance at LTI and 12.71 % at SB, and they were due to the vertical change of speed and direction of the currents, from the PCC to the PCUC.

Brochier et al. (2008a) in the South Eastern Pacific region and Brochier et al. (2008b) in the Canary Current System found that simulated anchovy larval retention increased with spawning depth and displayed a seasonal pattern

linked to the variability of subsurface current depth, in a similar way than in our results. Seasonal pattern of larval retention in LTI could be explained by the seasonal behavior of the PCC which reaches a minimum during austral Summer and Fall, and a maximum in austral Winter (Chaigneau et al., 2013; Echevin et al., 2011).

Simulation II showed that highest larval transport success values from SB to LTI were obtained at deeper spawning depth in summer due to the presence of stronger poleward subsurface countercurrents, favoring the larval transport from the bay to the island, which is not possible at shallow depths due to equatorward currents (Figure 3, upper panels, black squares). In summer, the northward surface flow associated to the PCC is reduced, whereas the poleward subsurface flow associated to the PCUC is enhanced (Figure 3; lower panel), as shown previously by Chaigneau et al. (2013). The interaction of month-depth factors was also important for larval transport, explaining 15.8 % of the variance.

Simulation IV showed a similar seasonal pattern of larval transport from LTI to SB. Even though the release depth of particles had a significant effect, the deepest release depth (30 - 45 m) presented lower transport than the intermediate release depth (15 - 30 m). Both, LTI and SB, presented the highest transport success at depths between 15 and 30 m, probably because at deeper depths northward currents are weaker (Figure 3; lower panel), and at shallower depths off-shore currents are stronger. The interaction of month-depth factors was also important for larval transport, explaining 13.61 % of the variance.

An enhanced upwelling south of the island in summer months allowed more particles to return to the island. In contrast, the downwelling pattern during

the winter months (Figure 9, right panels) may explain the almost null transport during this season. These results emphasize the importance of release location within SB on larval transport to LTI, highlighting the fact that the main historical natural banks in SB were located in the southern part of the bay whose larval transport trajectories arrive to the natural banks in the eastern side of LTI, so these historical natural banks should be protected as source of larvae for LTI.

Both seasonal patterns, larval retention and larval transport match the seasonal variation of gonadosomatic index of *A. purpuratus* (Figure 4, upper panels) described by Cisneros (2012). As a result of this match, weighting the number of virtual larvae released in the model would only reinforce the patterns emerging from hydrodynamics alone. The match of gonadosomatic index with the transport patterns that we found could indicate an evolutionary adaptation of the species to find the best conditions of food, temperature, and transport at the time of spawning. Testing for such hypothesis would need an adult fecundity model, as did Le Goff et al. (2017).

1.16. Future modelling perspectives

Higher spatial resolution models (e.g. from 2.2 km to 500 m) could allow to represent more precisely the bathymetry, circulation patterns, distribution of adult scallops, patchiness of spawning areas and larval transport pathways within the bay and close to the island. This would be useful for management purpose as it may allow to study transport variability within the spawning areas, thus allowing to identify optimal area for collecting and protecting the scallops (Liu et al., 2015).

Also, the inclusion of a bioenergetics submodel, e.g. DEB theory (Kooijman, 2010), will allow to calculate the mass, volume and buoyancy

changes of the larvae according to food and temperature. For this purpose, the hydrodynamic submodel should be coupled to a biogeochemical submodel, in order to obtain food inputs for the bioenergetics submodel, and scallop larvae buoyancy should be measured.

Modeling the environment dependent larval growth is an interesting perspective as this would modulate the pelagic larval duration (PLD), for example, temperature-dependent growth greatly impact seasonal transport patterns (Munroe et al., 2018). In northern Peru there is a strong temperature and salinity gradient separating TSW (Tropical Surface Waters) from ESW (Equatorial Surface Waters) in the first ~100 m of the water column (4 - 6 °S), which form the Equatorial Front (Pak et al., 1974; Zuta and Guillen, 1970); in addition, in summer there is a strong vertical temperature gradient with a thermocline centered at 30-40 m depth (off 5 °S), while in winter the vertical temperature gradient is weaker (Grados et al., 2018). These thermal gradients may have a significant effect on the growth of the larva and the duration of the PLD. In addition, Garavelli et al. (2014) found that with longer PLD, larval retention and subsequent settlement in a coastal upwelling area was lower, in line with our results.

In the present study, the vertical distribution of successful larvae (deeper pathways) differed from the vertical distribution of the majority of larvae that were lost (shallower pathways), and these results highlight the importance of further studies on vertical swimming speed and vertical distribution of *Argopecten purpuratus* larvae to implement vertical behaviors in the model, in order to assess which processes control larval behavior, vertical distribution and vertical migration amplitude. Other authors have implemented Diel Vertical

Migration (DVM) in fishes (Brochier et al., 2008a, 2008b), crustaceans (Carr et al., 2007; Peliz et al., 2007) and mollusks (Gilbert et al., 2010; Manuel et al., 1997, 1996, Nicolle et al., 2016, 2013, Tian et al., 2009a, 2009b). The inclusion of vertical migration in the model will allow to simulate larval vertical distribution in different hydrodynamic contexts, for example, with shallower migration depths we could expect a decrease in larval transport from SB to LTI and a decrease in local retention around LTI, due to the presence of northward surface currents; on the other hand, with deeper migration depths we could expect a higher larval transport from SB to LTI due to the presence of sub-surface currents in southward direction and a higher larval retention in LTI due to less intense current velocity. For other species of bivalves different settling velocities related to its larval stages have been reported (Mann et al., 1991), increasing the complexity of the vertical behavior. Furthermore, pediveliger larvae stay near the bottom before settlement searching for optimal substratum (Bandin and Mendo, 1999), so future models could also implement this behavior, which could be very sensitive to bottom currents (Koehl, 2007).

Although the OMZ in northern Peru is located at depths greater than 50 m (Bertrand et al., 2010), recent surveys in Sechura Bay showed frequent hypoxia and anoxia events at 10 m depth (Aguirre-Velarde, pers. comm.). In addition, anoxic conditions can also occur during extreme events, such as anomalous river discharges, harmful algal blooms or El Niño conditions. These conditions could become more frequent in the future in the context of climate change due to the projected expansion of the OMZ (Stramma et al., 2012, 2010; Ulloa et al., 2012), reducing the oxic habitat of scallops.

Scallop populations in Peru are affected by other factors than dispersal, for example, riverine discharge affects mortality of adults (Taylor et al. 2008), strong fishing pressure exerted on the seeds of LTI natural banks results in the permanent presence of individuals of smaller sizes than in SB (Mendo, 2009), and a decline in prices in foreign markets has led to an increase in export volumes in recent years (Mendo, 2009). These additional factors could be incorporated in more complex models. In addition, to better understand larval production variability it would be useful to analyze the spawning stock biomass using length-structured data, and to implement a larval monitoring system between and within both areas.

Marín et al. (2013), analyzed the genetic structure of three scallop populations in Peru: SB (5°40′ S), Samanco Bay (9°14’ S) and Independecia Bay (14°15’ S). They did not find significant differences in the genetic structures of these populations. This was attributed to a significant relocation of scallop spats from one region to another for aquaculture activities and/or larval flow connecting them. At a smaller spatial scale, we showed here that transport from SB to LTI was possible, and relocation of spats from the island to the bay is a common practice, thus both processes should contribute to panmixia. So, a gene flow study between scallop sub-populations along the Peruvian coast is necessary due to the potential translocation of spats, and the presence of small natural banks in San Lorenzo Island [12 °S] and Samanco Bay (9°14’ S) in Central Peru, which are located between Independencia Bay (14°15’ S) and LTI [6.4 °S], using elemental fingerprinting tracking (Becker et al., 2007) or DNA markers in mollusks (Ye et al., 2015).

The results obtained from this work have important consequences for natural banks and aquaculture co-management, especially in marine protected areas. The large proportion of local retention compared to transport in the larval supply to LTI, and the small area (6000 ha) of suitable habitat for scallop around the island, shows the importance of protecting the LTI natural banks to ensure self-retention of larvae and to avoid relocation of adults and mega-spawners from island subpopulation. Indeed, there is a long-term dominance of juveniles in the size structure of the population at LTI (Mendo com. pers.) and fishers do not relocate mega-spawners from the island due to their size (larger than 80 mm, while commercial scallop size is 65 mm), fragility and deep habitat, securing a minimum population level (Carbajal et al., 2005, 2004; De La Cruz et al., 2006; Ramirez et al., 2016).

On the other hand, as extreme events (related to environmental conditions or human perturbations) could eradicate the island subpopulation, it is necessary to restore and maintain the natural banks in SB too (Kluger et al., 2016; Tam et al., 2013). LTI and SB are the only two areas with historical natural populations of scallops in northern Peru. Tafur et al. (2000) reported that the scallop population in LTI almost disappeared in 1998 during the extreme El Niño event. However, mega-spawners reach deep habitats in SB, allowing them to survive during El Nino events. In this context, fishers have taken a first step towards the restoration and maintenance of natural banks in SB by establishing an agreement with the Regional Government to harvest a part of the commercial sized individuals and to leave another part unharvested as mega-spawners (Gobierno Regional de Piura, 2014a, 2014b). In addition, it is

necessary to estimate the difference between the recruitment minus the carrying capacity at LTI in order to assess the impact of translocation.

In addition, the amount of seed that could be translocated sustainably can be estimated as the difference between the recruitment minus the carrying capacity at LTI, which need to be estimated. Also, mega-spawners reach deep habitats in SB, allowing them to survive during El Nino events.

Finally, the knowledge gained about larval retention and transport trajectories using our simulations in this system, could be valuable to design potential location of spat collectors in the Northern part of the island or the Southern part of the bay to supply seeds for aquaculture activities.

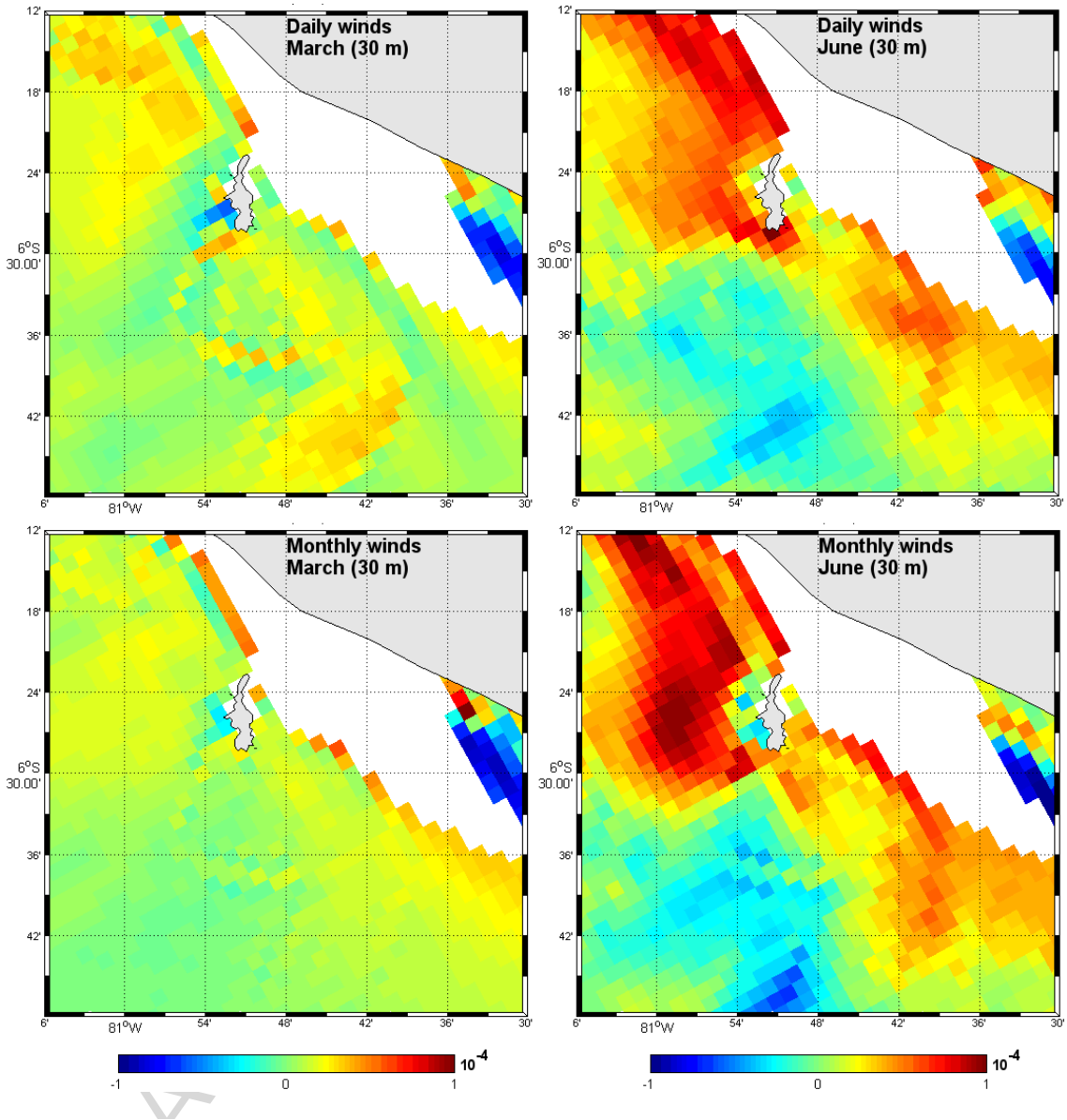

2. CONCLUSION

Larval supply of Peruvian scallop (*A. purpuratus*) to LTI simulated with a larval transport biophysical model comes from larval local retention at LTI (94.9 % of total supply and 2.4 % of total released) and larval transport from SB (5.1 % of total supply and 0.02 % of total released). Main factors maximizing larval retention and larval transport were spawning month (Dec-Apr) and spawning depth (30-45 m for retention and 20-30 m for transport). Retained particles followed counterclockwise trajectories in the eastern part of LTI, while transported particles from SB to LTI followed two main trajectories leaving the southern part of SB: one near the coast and arriving to the northern part of LTI, and the other far from the coast and arriving to the southern part of LTI. In future studies metapopulation dynamics should be taken into account by including the potential contribution of other banks, in order to test if SB could be considered as a 'source' population and LTI as a 'sink' population, as there is a net transport from SB to LTI.

Our results underline the importance of restoration and maintenance of both LTI and SB natural banks of Peruvian scallop: protecting the SB bank would ensure a source of larvae for LTI when environmental conditions or human perturbations jeopardize the island subpopulation; and protecting the LTI bank is also important as it has a high retention of larvae due to mesoscale processes.

Figure 9 Monthly mean vertical velocity (m/s) during a month with high larval transport (March; left panels) and low larval transport (June; right panels) for hydrodynamical model simulation forced by daily wind (upper panels) and

monthly climatological winds (lower panels). Positive vertical velocities correspond to upwelling. These upwelling cells southwest of the island allow the particles to rise and to return to the island through equatorward surface current. Similar vertical velocity patterns occur at 10 and 20 m depths (not shown).

ACKNOWLEDGMENTS:

We appreciate valuable discussions about scallop fishery, aquaculture and ecology with Maria Nelly Sanjinez and Juan Arguelles from IMARPE and with Martín Salazar from the Coastal Laboratory of Paita - IMARPE. We also thank Dimitri Gutierrez, from the General Research Direction of Oceanography and Climate Change and from the Master Program in Marine Science of Universidad Peruana Cayetano Heredia (UPCH). We acknowledge the support of the Science and Technology National Council (CONCYTEC – PERU) and the cooperative agreement between IMARPE and the Institut de Recherche pour le Développement (IRD) through the support of the JEAI "EMACEP" (Quantitative Marine Ecology of the Peruvian Upwelling Ecosystem) and the International Joint Laboratory LMI DISCOH (“Dynamics of the Humboldt Current System”). Finally, we thank the permanent feedback from the staff of the Laboratory of Oceanographical, Ecosystem and Climate Change Modelling of IMARPE.

REFERENCES

Aguirre-Velarde, A., 2016. Bioenergetics of the Peruvian scallops (*Argopecten purpuratus*) in an environmental context limiting oxygen. Université de Bretagne Occidentale. Available in: https://tel.archives-ouvertes.fr/tel-01542077/document.

Bandin, R., Mendo, J., 1999. Asentamiento larval de la concha de abanico (*Argopecten purpuratus*) en colectores artificiales en la Bahía Independencia, Pisco, Perú. Investig. Mar. 27, 3–13. doi:10.4067/S0717-71781999002700001

Becker, B.J., Levin, L.A., Fodrie, F.J., McMillan, P.A., 2007. Complex larval connectivity patterns among marine invertebrate populations. Proc. Natl. Acad. Sci. 104, 3267–3272. doi:10.1073/pnas.0611651104

Becker, J.J., Sandwell, D.T., Smith, W.H.F., Braud, J., Binder, B., Depner, J., Fabre, D., Factor, J., Ingalls, S., Kim, S.-H., Ladner, R., Marks, K., Nelson, S., Pharaoh, A., Trimmer, R., Von Rosenberg, J.,

Wallace, G., Weatherall, P., 2009. Global Bathymetry and Elevation Data at 30 Arc Seconds Resolution: SRTM30_PLUS. Mar. Geod. 32, 355–371. doi:10.1080/01490410903297766

Bentamy, A., Fillon, D.C., 2012. Gridded surface wind fields from Metop / ASCAT measurements. Int. J. Remote Sens. 33, 1729–1754.

Bertrand, A., Ballón, M., Chaigneau, A., 2010. Acoustic Observation of Living Organisms Reveals the Upper Limit of the Oxygen Minimum Zone. PLoS One 5, e10330. doi:10.1371/journal.pone.0010330

Brochier, T., Lett, C., Tam, J., Fréon, P., Colas, F., Ayón, P., 2008a. An individual-based model study of anchovy early life history in the northern Humboldt Current system. Prog. Oceanogr. 79, 313–325. doi:10.1016/j.pocean.2008.10.004

Brochier, T., Ramzi, A., Lett, C., Machu, E., Berraho, A., Fréon, P., Hernández-León, S., 2008b. Modelling sardine and anchovy ichthyoplankton transport in the Canary Current System. J. Plank. Res. 30, 1133–1146. doi:10.1093/plankt/fbn066

Bryan-Brown, D.N., Brown, C.J., Hughes, J.M., Connolly, R.M., 2017. Patterns and trends in marine population connectivity research. Mar. Ecol. Prog. Ser. 585, 243–256. doi:10.3354/meps12418

Carbajal, W., De la Cruz, J., Ramirez, P., Bances, S., Galán, J., Castañeda, J., 2005. Evaluación poblacional del recurso concha de Abanico *Argopecten purpuratus* en la Isla Lobos de Tierra (6 – 12 enero 2005). Santa Rosa - Chiclayo. Available in: http://www.imarpe.gob.pe/chiclayo/informes/Inf%20Concha%20abanico%20ILT%20Ene%2005.pdf.

Carbajal, W., De la Cruz, J., Ramirez, P., Castro, J., Bances, S., 2004. Evaluación poblacional del recurso concha de abanico *Argopecten purpuratus* en la Isla Lobos de Tierra (3 – 8 de enero 2004). Ins. del Mar del Peru - Santa Rosa - Chiclayo. Availablein:http://www.imarpe.gob.pe/chiclayo/informes/Informe%20Evaluacion%20de%20concha%20de%20abanico%20Enero%202004.pdf.

Carr, S.D., Capet, X.J., McWilliams, J.C., Pennington, J.T., Chavez, F.P., 2007. The influence of diel vertical migration on zooplankton transport and recruitment in an upwelling region: Estimates from a coupled behavioral-physical model. Fish. Oceanogr. 17, 1–15. doi:10.1111/j.1365-2419.2007.00447.x

Chaigneau, A., Dominguez, N., Eldin, G., Vasquez, L., Flores, R., Grados, C., Echevin, V., 2013. Near-coastal circulation in the Northern Humboldt Current System from shipboard ADCP data. J. Geophys. Res. Ocean. 118, 5251–5266. doi:10.1002/jgrc.20328

Cisneros, R., 2012. Estudio Bio-oceanográfico para determinación de la capacidad de carga en la Bahía de Sechura - IMARPE - Informe Final. Callao. Available in: http://rnia.produce.gob.pe/images/stories/archivos/pdf/publicaciones/informe_final_capacidad_de_carga_sechura.pdf.

Colas, F., McWilliams, J.C., Capet, X., Kurian, J., 2012. Heat balance and eddies in the Peru-Chile current system. Clim. Dyn. 39, 509–529. doi:10.1007/s00382-011-1170-6

Cragg, S.M., 2016. Biology and ecology of scallop larvae, in: Shumway, S., Parsons, J. (Eds.), Scallops: Biology, Ecology, Aquaculture, and Fisheries. pp. 31–83.

Cragg, S.M., 2006. Development, physiology, behaviour and ecology of scallop larvae, in: Shumway, S., Parsons, J. (Eds.), Scallops: Biology, Ecology, Aquaculture, and Fisheries. pp. 45–122. doi:10.1016/S0167-9309(06)80029-3

Cragg, S.M., 1980. Swimming behaviour of the larvae of Pecten maximus (L.) (Bivalvia). J. Mar. Biol. Assoc. UK 60, 551–564. doi:10.1017/S002531540004025X

Da Silva, A.M., Young, C.C., Levitus, S., 1994. Atlas of surface marine data 1994, in: Algorithms and Procedures, Technical Report. NOAA Atlas Nesdis. p. 74.

De La Cruz, J., Ramirez, P., Bances, S., Carbajal, W., 2006. Evaluación poblacional del recurso *Argopecten purpuratus* concha de abanico en la isla lobos de tierra (28 abril – 02 mayo 2006). Chiclayo - Santa Rosa. Available in: http://www.imarpe.gob.pe/chiclayo/informes/Inf%20Eval%20Pob%20Concha%20Abanico%20Isla%20Lobos%20Tierra,%20Abril%202006.pdf.

Echevin, V., Colas, F., Chaigneau, A., Penven, P., 2011. Sensitivity of the Northern Humboldt Current System nearshore modeled circulation to initial and boundary conditions. J. Geophys. Res. Ocean. 116, 1–16. doi:10.1029/2010JC006684

Garavelli, L., Kaplan, D.M., Colas, F., Stotz, W., Yannicelli, B., Lett, C., 2014. Identifying appropriate spatial scales for marine conservation and management using a larval dispersal model: The case of Concholepas concholepas (loco) in Chile. Prog. Oceanogr. 124, 42–53. doi:10.1016/j.pocean.2014.03.011

Gilbert, C.S., Gentleman, W.C., Johnson, C.L., Dibacco, C., Pringle, J.M., Chen, C., 2010. Progress in Oceanography Modelling dispersal of sea scallop (Placopecten magellanicus) larvae on Georges Bank : The influence of depth-distribution , planktonic duration and spawning seasonality. Prog. Oceanogr. 87, 37–48. doi:10.1016/j.pocean.2010.09.021

Gobierno Regional de Piura, 2014a. Resolución Directoral Regional N° 309-2014. Piura.Available in: http://direpro.regionpiura.gob.pe/documentos/resoluciones/res309_2014.pdf.

Gobierno Regional de Piura, 2014b. Resolución Directoral Regional N° 202-2014. Piura.Available in: http://direpro.regionpiura.gob.pe/documentos/resoluciones/res202_2014.pdf.

Grados, C., Chaigneau, A., Echevin, V., Dominguez, N., 2018. Upper ocean hydrology of the Northern Humboldt Current System at seasonal, interannual and interdecadal scales. Prog. Oceanogr. 165, 123–144. doi:10.1016/j.pocean.2018.05.005

Grimm, V., Berger, U., Bastiansen, F., Eliassen, S., Ginot, V., Giske, J., Goss-Custard, J., Grand, T., Heinz, S.K., Huse, G., Huth, A., Jepsen, J.U., Jørgensen, C., Mooij, W.M., Müller, B., Pe'er, G., Piou, C., Railsback, S.F., Robbins, A.M., Robbins, M.M., Rossmanith, E., Rüger, N., Strand, E., Souissi, S., Stillman, R.A., Vabø, R., Visser, U., DeAngelis, D., 2006. A standard protocol for describing individual-based and agent-based models. Ecol. Model. 198, 115–126. doi:10.1016/j.ecolmodel.2006.04.023

Grimm, V., Berger, U., DeAngelis, D., Polhill, J.G., Giske, J., Railsback, S.F., 2010. The ODD protocol: A review and first update. Ecol. Model. 221, 2760–2768. doi:10.1016/j.ecolmodel.2010.08.019

Hanski, I., Gilpin, M., 1991. Metapopulation dynamics : brief history and conceptual domain. Biol. J. Linn. Soc. 42, 3–16.

Jonsson, P.R., Berntsson, K.M., Larsson, A.I., 2004. Linking larval supply to recruitment: Flow-mediated control of initial adhesion of barnacle larvae. Ecology 85, 2850–2859. doi:10.1890/03-0565

Kämpf, J., Chapman, P., 2016. The Peruvian-Chilean Coastal Upwelling System, in: Upwelling Systems of the World. Springer, pp. 161–201. doi:10.1007/978-3-319-42524-5

Kluger, L.C., Taylor, M.H., Mendo, J., Tam, J., Wolff, M., 2016. Carrying capacity simulations as a tool for ecosystem-based management of a scallop aquaculture system. Ecol. Model. 331, 44–55. doi:10.1016/j.ecolmodel.2015.09.002

Kluger, L.C., Taylor, M.H., Wolff, M., Stotz, W., Mendo, J., 2018. From an open-access fishery to a regulated aquaculture business: the case of the most important Latin American bay scallop (*Argopecten purpuratus*). Rev. Aquac. 1–17. doi:10.1111/raq.12234

Koehl, M.R.A., 2007. Mini review: Hydrodynamics of larval settlement into fouling communities. Biofouling 23, 357–368. doi:10.1080/08927010701492250

Kooijman, S.A.L.M., 2010. Dynamic Energy Budget theory for metabolic organisation, third edit. ed. Vrije Universiteit, Amsterdam, Amsterdam. doi:10.1098/rstb.2010.0167

Large, W.G., McWilliams, J.C., Doney, S.C., 1994. Ocean vertical mixing: a review and a model with a non-local boundary layer parameterization. Rev. Geophys. 32, 363–404.

Le Goff, C., Lavaud, R., Cugier, P., Jean, F., Flye-Sainte-Marie, J., Foucher, E., Desroy, N., Fifas, S., Foveau, A., 2017. A coupled biophysical model for the distribution of the great scallop Pecten maximus in the English Channel. J. Mar. Syst. 167, 55–67. doi:10.1016/j.jmarsys.2016.10.013

Lett, C., Nguyen-Huu, T., Cuif, M., Saenz-Agudelo, P., Kaplan, D.M., 2015. Linking local retention, self-recruitment, and persistence in marine metapopulations. Ecology 96, 2236–2244. doi:10.1890/14-1305.1

Lett, C., Verley, P., Mullon, C., Parada, C., Brochier, T., Penven, P., Blanke, B., 2008. A Lagrangian tool for modelling ichthyoplankton dynamics. Environ. Model. Softw. 23, 1210–1214. doi:10.1016/j.envsoft.2008.02.005

Lindo-Atichati, D., Curcic, M., Paris, C.B., Buston, P.M., 2016. Description of surface transport in the region of the Belizean Barrier Reef based on observations and alternative high-resolution models. Ocean Model. 106, 74–89. doi:10.1016/j.ocemod.2016.09.010

Liu, C., Cowles, G.W., Churchill, J.H., Stokesbury, K.D.E., 2015. Connectivity of the bay scallop (Argopecten irradians) in Buzzards Bay, Massachusetts, U.S.A. Fish. Oceanogr. 24, 364–382. doi:10.1111/fog.12114

Mann, R., Campos, B.M., Luckenbach, M.W., 1991. Swimming rate and responses of larvae of three mactrid bivalves to salinity dicontinuities. Mar. Ecol. Prog. Ser. 68, 257–269. doi:10.3354/meps068257

Manuel, J.L., Gallager, S.M., Pearce, C.M., Manning, D.A., O'Dor, R.K., 1996. Veligers from different populations of sea scallop Placopecten magellanicus have different vertical migration patterns. Mar. Ecol. Prog. Ser. 142, 147–163. doi:10.3354/meps142147

Manuel, J.L., Pearce, C.M., O'Dor, R.K., 1997. Vertical migration for horizontal transport while avoiding predators: II. Evidence for the tidal/diel model from two populations of scallop (Placopecten magellanicus) veligers. J. Plankt. Reseasrch 19, 1949–1973.

Marín, A., Fujimoto, T., Arai, K., 2013. Genetic structure of the Peruvian scallop *Argopecten purpuratus* inferred from mitochondrial and nuclear DNA variation. Mar. Genomics 9, 1–8. doi:10.1016/j.margen.2012.04.007

Mason, E., Molemaker, J., Shchepetkin, A.F., Colas, F., Mcwilliams, J.C., Sangrà, P., 2010. Procedures for offline grid nesting in regional ocean models. Ocean Model. 35, 1–15. doi:10.1016/j.ocemod.2010.05.007

McWilliams, J.C., Colas, F., Molemaker, M.J., 2009. Cold filamentary intensification and oceanic surface convergence lines. Geophys. Res. Lett. 36, 1–5. doi:10.1029/2009GL039402

Mendo, J., 2009. Asistencia técnica para la evaluación del potencial de stocks de conchas de abanico. Lima. Available in: http://humboldt.iwlearn.org/es/informacion-y-publicacion/MINCETUR2010evaluacionpotencialconchaabanicoPeruMendo.pdf.

Mendo, J., Wolff, M., Mendo, T., Ysla, L., 2016. Scallop Fishery and Culture in Peru, in: Shumway, S., Parsons, J. (Eds.), Scallops: Biology, Ecology, Aquaculture, and Fisheries. pp. 1089–1109. doi:10.1016/B978-0-444-62710-0.00028-6

Mendo, J., Yamashiro, C., Rubio, J., Kameya, A., Jurado, E., Maldonado, M., Guzmán, S., 1989. Evaluacion de la población de concha de abanico (*Argopecten purpuratus*) en la bahía Independencia, Pisco, Perú, 23 de Setiembre - 9 de Octubre de 1987. Lima. Available in:http://biblioimarpe.imarpe.gob.pe/bitstream/123456789/2039/1/INF%2094.pdf.

Mendo, J., Ysla, L., Orrego, H., Miglio, M., Gil, P., Del Solar, A., 2011. Manual técnico para el repoblamiento de concha de abanico en la Bahía de Sechura.

Miller, T.J., 2007. Contribution of individual-based coupled physical-biological models to understanding recruitment in marine fish populations. Mar. Ecol. Prog. Ser. 347, 127–138. doi:10.3354/meps06973

MINAM, 2009. DECRETO SUPREMO N° 024-2009: Decreto supremo que aprueba el estableciemitno de la reserva nacional sistema de islas, islotes y puntas guaneras. Lima. Available in: http://www.sernanp.gob.pe/sistema-de-islas-islotes-y-puntas-guaneras.

Monin, A.S., Ozmidov, R.V., 1985. Turbulence in the Ocean. doi:10.1017/CBO9781107415324.004

Morón, O., Velazco, F., Beltran, L., 2013. Caracteristicas hidrograficas y sedimentologicas de la Bahia de Sechura, Instituto del Mar del Perú - INFORME. Callao. Available in: http://biblioimarpe.imarpe.gob.pe:8080/handle/123456789/2238.

Munroe, D.M., Haidvogel, D., Caracappa, J.C., Klinck, J.M., Powell, E.N., Hofmann, E.E., Shank, B. V., Hart, D.R., 2018. Modeling larval dispersal and connectivity for Atlantic sea scallop (Placopecten magellanicus) in the Middle Atlantic Bight. Fish. Res. 208, 7–15. doi:10.1016/j.fishres.2018.06.020

Nicolle, A., Dumas, F., Foveau, A., Foucher, E., Thiébaut, E., 2013. Modelling larval dispersal of the king scallop (Pecten maximus) in the English Channel : examples from the bay of Saint-Brieuc and the bay of Seine. Ocean Dyn. 661–678. doi:10.1007/s10236-013-0617-1

Nicolle, A., Moitie, R., Ogor, J., Dumas, F., Foucher, E., Thie, E., Marin, M., 2016. Modelling larval dispersal of Pecten maximus in the English Channel : a tool for the spatial management of the stocks. ICES J. Mar. Sci. doi:10.1093/icesjms/fsw207

Pak, H., Zaneveld, J.R. V., Pak, H., Zaneveld, J.R. V., 1974. Equatorial Front in the Eastern Pacific Ocean. J. Phys. Oceanogr. 4, 570–578.

Peck, M.A., Hufnagl, M., 2012. Can IBMs tell us why most larvae die in the sea? Model sensitivities and scenarios reveal research needs. J. Mar. Syst. 93, 77–93. doi:10.1016/j.jmarsys.2011.08.005

Peliz, A., Marchesiello, P., Dubert, J., Marta-Almeida, M., Roy, C., Queiroga, H., 2007. A study of crab larvae dispersal on the Western Iberian Shelf: Physical processes. J. Mar. Syst. 68, 215–236. doi:10.1016/j.jmarsys.2006.11.007

Penven, P., Echevin, V., Pasapera, J., Colas, F., Tam, J., 2005. Average circulation, seasonal cycle, and mesoscale dynamics of the Peru Current System: A modeling approach. J. Geophys. Res. C Ocean. 110, 1–21. doi:10.1029/2005JC002945

Pineda, J., 2000. Linking larval settlement to larval transport: Assumptions, potentials, and pitfalls. Oceanogr. East. Pacific 1, 84–105.

Pineda, J., Hare, J., Sponaugle, S., 2007. Larval Transport and Dispersal in the Coastal Ocean and Consequences for Population Connectivity. Oceanography 20, 22–39.

PRODUCE, 2016. Anuario Estadístico Pesquero y Acuícola. Lima. Available in: https://www.produce.gob.pe/documentos/estadisticas/anuarios/anuario-estadistico-pesca-2015.pdf.

Ramirez, P., De la Cruz, J., Castro, J., 2016. Evaluación poblacional de *Argopecten purpuratus*, Transennella pannosa y prospección de Octopus mimus. Isla Lobos de Tierra, 2015. Callao. Available in: http://biblioimarpe.imarpe.gob.pe:8080/handle/123456789/3115.

Shchepetkin, A.F., McWilliams, J.C., 2005. The regional oceanic modeling system (ROMS): A split-explicit, free-surface, topography-following-coordinate oceanic model. Ocean Model. 9, 347–404. doi:10.1016/j.ocemod.2004.08.002

Stotz, W., 2000. When aquaculture restores and replaces an overfished stock:Is the conservation of the Species assured? The case of the scallop *Argopecten purpuratus* in Northern Chile. Aquac. Int. 8, 237–247. doi:10.1023/A:1009215119051

Stramma, L., Prince, E.D., Schmidtko, S., Luo, J., Hoolihan, J.P., Visbeck, M., Wallace, D.W.R., Brandt, P., Körtzinger, A., 2012. Expansion of oxygen minimum zones may reduce available habitat for tropical pelagic fishes. Nat. Clim. Chang. 2, 33–37. doi:10.1038/nclimate1304

Stramma, L., Schmidtko, S., Levin, L., Johnson, G.C., 2010. Ocean oxygen minima expansions and their biological impacts. Deep. Res. Part I Oceanogr. Res. Pap. 57, 587–595. doi:10.1016/j.dsr.2010.01.005

Tafur, R., Castillo, G., Taipe, A., Vásquez, L., Delgado, E., Carrasco, N., 2000. Evaluacion poblacional de la concha de abanico (Argopeten purpuratus) en Bahia de Sechura e Isla Lobos de Tierra. Julio 1999. Callao.Available in: http://biblioimarpe.imarpe.gob.pe:8080/handle/123456789/1434.

Tam, J., Espinoza, D., Oliveros, R., Romero, C., Ramos, J., 2013. Modelos de simulación y determinación de la capacidad de carga de la concha de abanico *Argopecten purpuratus*, in: IMARPE (Ed.), IMARPE. Estudio Bio-Oceanográfico Para Determinación de La Capacidad de Carga En La Bahía Sechura. Informe Interno Inst. Mar Perú. Lima.

Taylor, M., Wolff, M., Vadas, F., Yamashiro, C., 2008. Trophic and environmental drivers of the sechura bay ecosystem (Peru) over an ENSO cycle. Helgol. Mar. Res. 62, 15–32. doi:10.1007/s10152-007-0093-4

Thomsen, S., Kanzow, T., Colas, F., Echevin, V., Krahmann, G., Engel, A., 2016. Do submesoscale frontal processes ventilate the oxygen minimum zone off Peru? Geophys. Res. Lett. 43, 8133–8142. doi:10.1002/2016GL070548

Tian, R., Chen, C., Stokesbury, K.D.E., Rothschild, B.J., Cowles, G.W., Xu, Q., Hu, S., Harris, B.P., Marino II, M., 2009a. Modeling the connectivity between sea scallop populations in the Middle Atlantic Bight and over Georges Bank. Mar. Ecol. Prog. Ser. 380, 147–160. doi:10.3354/meps07916

Tian, R., Chen, C., Stokesbury, K.D.E., Rothschild, B.J., Cowles, G.W., Xu, Q., Hu, S., Harris, B.P., Marino, M.C., 2009b. Dispersal and settlement of sea scallop larvae spawned in the fishery closed areas on Georges Bank. ICES J. Mar. Sci. 66, 2155–2164. doi:10.1093/icesjms/fsp175

Ulloa, O., Canfield, D.E., DeLong, E.F., Letelier, R.M., Stewart, F.J., 2012. Microbial oceanography of anoxic oxygen minimum zones. Proc. Natl. Acad. Sci. 109, 15996–16003. doi:10.1073/pnas.1205009109

von Brand, E., Merino, G.E., Abarca, A., Stotz, W., 2006. Chapter 27 Scallop fishery and aquaculture in Chile. Dev. Aquac. Fish. Sci. 35, 1293–1314. doi:10.1016/S0167-9309(06)80054-2

Wolff, M., 1988. Spawning and recruitment in the Peruvian scallop *Argopecten purpuratus*. Mar. Ecol. Prog. Ser. 42, 213–217. doi:10.3354/meps042213

Wolff, M., 1987. Population dynamics of the Peruvian scalop *Argopecten purpuratus* during the El Niño Phenomenon of 1983. Can. J. Fish. Aquat. Sci. 44, 1684–1691. doi:10.1139/f87-207

Wolff, M., Taylor, M., Mendo, J., Yamashiro, C., 2007. A catch forecast model for the Peruvian scallop (*Argopecten purpuratus*) based on estimators of spawning stock and settlement rate. Ecol. Model. 209, 333–341. doi:10.1016/j.ecolmodel.2007.07.013

Ye, Y.Y., Wu, C.W., Li, J.J., 2015. Genetic population structure of Macridiscus multifarius (mollusca: Bivalvia) on the basis of mitochondrial markers: Strong population structure in a species with a short planktonic larval stage. PLoS One 10, 1–13. doi:10.1371/journal.pone.0146260

Zuta, S., Guillen, O., 1970. Oceanografia de las Aguas Costeras del Perú. Lima. Ins. del Mar del Peru

Table 1 Set of parameters tested in each particles transport simulations.

	Simulation I	**Simulation II**
Objective	Larval retention in LTI	Larval transport from SB to LTI
Spawning zone	Lobos de Tierra (~6.3 °S)	Sechura (~5 °S)
Settlement zone	Lobos de Tierra (~6.3 °S)	Lobos de Tierra (~6.3 °S)
Spawning month	each month	each month
Spawning depth (m)	0-15;15-30;30-45	0-10;10-20;20-30
Minimum age to settlement (days)	15;20;25	15;20;25

	Simulation III	**Simulation IV**
Objective	Larval retention in SB	Larval transport from LTI to SB
Spawning zone	Sechura (~5 °S)	Lobos de Tierra (~6.3 °S)
Settlement zone	Sechura (~5 °S)	Sechura (~5 °S)
Spawning month	each month	each month
Spawning depth (m)	0-10;10-20;20-30	0-15;15-30;30-45
Minimum age to settlement (days)	15;20;25	15;20;25

Table 2 Summary of PERMANOVA for larval retention simulations at LTI. Factors represent Year (of simulation), Month (of spawning), Depth (of spawning), and Age (minimum to settlement).

	Df	*Sum Sq*	*F value*	*Pr(>F)*	*%Exp*
year	2	105.781	2.257	0.040	0.378
month	11	5795.701	22.485	0.010	20.736
depth	2	5363.557	114.445	0.010	19.190
age	2	1887.653	40.278	0.010	6.754
year x month	22	2488.097	4.826	0.010	8.902
year x depth	4	162.877	1.738	0.070	0.583
year x age	4	36.295	0.387	0.910	0.130
month x depth	22	3643.683	7.068	0.010	13.036
month x age	22	1425.897	2.766	0.010	5.102
depth x age	4	1697.914	18.115	0.010	6.075
residuals	228	5342.690			19.115

Table 3 Summary of PERMANOVA for larval transport simulations from SB to LTI. Factors represent Year (of simulation), Month (of spawning), Depth (of spawning) and Age (minimum to settlement).

	Df	*Sum Sq*	*F value*	*Pr(>F)*	*%Exp*
year	2	0.130	4.834	0.010	1.069
month	11	2.532	17.146	0.010	20.855
depth	2	0.883	32.885	0.010	7.273
age	2	0.057	2.133	0.080	0.472
year x month	22	3.132	10.606	0.010	25.800
year x depth	4	0.102	1.894	0.050	0.838
year x age	4	0.018	0.330	0.970	0.146
month x depth	22	1.928	6.529	0.010	15.882
month x age	22	0.255	0.864	0.710	2.103
depth x age	4	0.043	0.793	0.550	0.351
residuals	228	3.061			25.212

Table 4 Summary of PERMANOVA for larval retention simulations at SB. Factors represent Year (of simulation), Month (of spawning), Depth (of spawning), and Age (minimum to settlement).

	Df	*Sum Sq*	*F value*	*Pr(>F)*	*%Exp*
year	2	101.852	4.664	0.010	1.523
month	11	644.188	5.363	0.010	9.630
depth	2	548.644	25.122	0.010	8.202
age	2	291.638	13.354	0.010	4.360
year x month	22	825.567	3.436	0.010	12.342
year x depth	4	111.985	2.564	0.010	1.674
year x age	4	65.619	1.502	0.150	0.981
month x depth	22	850.315	3.540	0.010	12.712
month x age	22	407.358	1.696	0.010	6.090
depth x age	4	352.345	8.067	0.010	5.267
residuals	228	2489.715			37.220

Table 5 Summary of PERMANOVA for larval transport simulations from LTI to SB. Factors represent Year (of simulation), Month (of spawning), Depth (of spawning) and Age (minimum to settlement).

	Df	*Sum Sq*	*F value*	*Pr(>F)*	*%Exp*
year	2	0.260	8.185	0.010	2.701
month	11	1.330	7.601	0.010	13.796
depth	2	0.145	4.568	0.010	1.507
age	2	0.048	1.523	0.140	0.502
year x month	22	2.332	6.666	0.010	24.198
year x depth	4	0.205	3.220	0.010	2.125
year x age	4	0.073	1.152	0.260	0.760
month x depth	22	1.312	3.750	0.010	13.614
month x age	22	0.269	0.768	0.960	2.787
depth x age	4	0.037	0.586	0.920	0.387
residuals	228	3.626			37.621

Highlights

- Larval transport model of Peruvian scallop simulated retention and transport between two natural banks in Northern Peru.
- Larval retention and larval transport of Peruvian scallop increased with spawning depth and were highest in austral summer.
- Larval transport trajectories between the two natural banks depended on complex mesoscale circulation patterns and vertical flows.
- Daily and monthly wind forcings changed simulated mean larval transport but retention was not affected.
- Restoration and maintenance of both natural banks will improve sustainability of aquaculture activities.